Distribution and Function of AP-1 Clathrin Adaptor Complexes in Polarized Epithelial Cells

Heike Fölsch,* Marc Pypaert,* Peter Schu,‡ and Ira Mellman*

*Department of Cell Biology and Ludwig Institute for Cancer Research, Yale University School of Medicine, New Haven, Connecticut 06520; and ‡Center for Biochemistry and Molecular Cell Biology, Biochemistry Department II, University of Göttingen, D-37073 Göttingen, Germany

Abstract. Expression of the epithelial cell–specific heterotetrameric adaptor complex AP-1B is required for the polarized distribution of many membrane proteins to the basolateral surface of LLC-PK1 kidney cells. AP-1B is distinguished from the ubiquitously expressed AP-1A by exchange of its single 50-kD μ subunit, μ1A, being replaced by the closely related μ1B. Here we show that this substitution is sufficient to couple basolateral plasma membrane proteins, such as a low-density lipoprotein receptor (LDLR), to the AP-1B complex and to clathrin. The interaction between LDLR and AP-1B is likely to occur in the trans-Golgi network (TGN), as was suggested by the localization of functional, epitope-tagged μ1 by immunofluorescence and immunoelectron microscopy. Tagged AP-1A and AP-1B complexes were found in the perinuclear region close to the Golgi complex and recycling endosomes, often in clathrin-coated buds and vesicles. Yet, AP-1A and AP-1B localized to different subdomains of the TGN, with only AP-1A colocalizing with furin, a membrane protein that uses AP-1 to recycle between the TGN and endosomes. We conclude that AP-1B functions by interacting with its cargo molecules and clathrin in the TGN, where it acts to sort basolateral proteins from proteins destined for the apical surface and from those selected by AP-1A for transport to endosomes and lysosomes.

Key words: cell polarity • Golgi complex • furin • trans-Golgi network • endosomes

Introduction

Epithelial cells generate and maintain at least two biochemically distinct plasma membrane domains that reside within a continuous lipid bilayer (Rodriguez-Boulan and Powell, 1992; Drubin and Nelson, 1996; Yeaman et al., 1999). The polarized distribution of membrane proteins and lipids to the apical or basolateral domain depends on several factors. First, most epithelial cells have the ability to sort newly synthesized plasma membrane components as they exit the TGN and package them into transport vesicles that are delivered to the correct target membrane. Second, to ensure that this polarized distribution is maintained despite rapid endocytosis at both the apical and basolateral surfaces, endosomes in epithelial cells are likewise capable of polarized sorting and transport to allow for recycling of internalized proteins and lipids to their correct domains. Finally, some membrane proteins may achieve polarity by selective retention at the apical or basolateral surface. Although less well understood, this may reflect interactions with extracellular ligands or with intracellular

scaffolds, such as cytoskeletal elements or arrays of PDZ domain–containing proteins (Mays et al., 1995; Cohen et al., 1998; Setou et al., 2000). For each of these mechanisms, polarity depends critically on the existence of specific signals encoded within the membrane proteins themselves.

It is well established that distinct types of signals determine apical versus basolateral sorting on the endocytic and secretory pathways. Apical sorting is thought to reflect selective segregation into glycolipid- and cholesterol-enriched raft domains, facilitated by the presence of critical N- or O-linked carbohydrate moieties in a protein's extracellular region or by the physical properties of the transmembrane domain (Scheiffele et al., 1995; Simons and Ikonen, 1997). Basolateral sorting signals are far better understood and frequently lie in a membrane protein's cytoplasmic domain (Matter and Mellman, 1994; Mostov et al., 1999; Matter, 2000). When present, they are also generally cis-dominant to apical signals. Although basolateral signals can contain critical tyrosine or di-leucine residues, their sequence motif appears to be degenerate, with no universal consensus or features having as yet emerged. It is nevertheless intriguing that these signals are similar to the tyrosine and dileucine-based signals which specify inclusion

in clathrin-coated vesicles at the plasma membrane or in the TGN. Such signals are known to interact with well characterized clathrin-associated adaptor complexes (Hirst and Robinson, 1998; Bonifacino and Dell'Angelica, 1999).

Adaptor complexes are heterotetrameric complexes that comprise two large, one medium, and one small subunit. By yeast two-hybrid and structural analysis, it is the medium or μ subunit that interacts with at least tyrosine-based sorting signals (Ohno et al., 1995, 1996; Owen and Evans, 1998). So far, several families of adaptor complexes (AP-1A/AP-1B, AP-2, AP-3A/AP-3B, and AP-4) have been described, one of them being the epithelial cell–specific AP-1B complex (Hirst and Robinson, 1998; Bonifacino and Dell'Angelica, 1999; Dell'Angelica et al., 1999a; Fölsch et al., 1999; Hirst et al., 1999; Ohno et al., 1999). AP-1B shares with the ubiquitously expressed AP-1A complex the large and small subunits, but contains its own medium subunit, μ1B. We have found recently that AP-1B (γ, β1, μ1B, σ1) is required for the proper polarity of many basolateral membrane proteins, with the mistargeting seen in μ1B-deficient LLC-PK1 porcine kidney epithelial cells corrected by transfection of a μ1B cDNA (Fölsch et al., 1999).

Each adaptor complex has a characteristic distribution in the cell that belies its function and signal selectivity. AP-2 complexes are found primarily at the plasma membrane, where they interact with cell surface receptors to concentrate them in clathrin-coated pits. AP-1, or at least AP-1A, complexes are found in the TGN and to a lesser extent in endosomes. Here, via their μ1A subunits, they interact with cargo such as mannose 6-phosphate receptor, leading to accumulation in clathrin-coated buds and transport to endosomes. AP-3 complexes are similarly distributed since they also bind lysosome-directed cargo and mediate transport to endocytic organelles with or without involving clathrin (Simpson et al., 1996; Dell'Angelica et al., 1998; Drake et al., 2000). We have now examined the cargo specificity and distribution of AP-1B complexes. Although similar to AP-1A complexes in general, with respect to intracellular localization and association with clathrin AP-1B complexes can be found to interact biochemically with basolateral targeting signals and, seemingly, to define a domain of the TGN distinct from that defined by AP-1A.

Materials and Methods

Cloning of HA-tagged μ1A and μ1B

Hemagglutinin (HA)[1]-tagged versions of μ1A and μ1B were cloned by PCR using mouse μ1A cDNA (sequence data available from EMBL/GenBank/DDBJ under accession no. M62419) or human μ1B cDNA (ID 123283; IMAGE consortium, Lawrence Livermore National Laboratory) as templates and the plaque forming unit (pfu)-polymerase (Stratagene). The internal HA tags were introduced into μ1A and μ1B between amino acids 230 and 231. First, the COOH termini were amplified using 5′-GCGCGAATTCATCGATGTGGAGCTGGAGGATGTGAAATTC-3′ and 5′-GCGCAAGCTTTCACTGGGTCCGGAGCTG-3′ as NH$_2$- and COOH-terminal primers, respectively, for μ1A; 5′-GCGCGAATTCATCGATGTAGAGCTGGAGGATGTAAAATTC-3′ as NH$_2$-terminal primer combined with 5′-GCGCAAGCTTCTAGCTGGTACGAAGGTTG-3′ as COOH-terminal primer were used for μ1B. Both fragments were cloned into pCB6 as EcoRIHindIII fragments. In a second

PCR reaction the NH$_2$-termini of both proteins were amplified using 5′-GCGCGAATTCCTCGAGATGTCCGCCAGCGCCGTCTACGTA-3′ as NH$_2$-terminal primer and 5′-GCGCATCGATGGCGTAGTCTGG-GACGTCGTATGGGTATGACTTGCTCTTCCCTCGGCCTGT-3′ as COOH-terminal primer, respectively, for μ1A cloning. For cloning of μ1B, the NH$_2$ terminal primer 5′-GCGCGAATTCCTCGAGATGTCCGCCTCGGCTGTCTTCATT-3′ and the COOH-terminal primer 5′-GCGCATCGATGGCGTAGTCTGTAGGGTATGAT-TTGTTCTTGCTGCGGCCAGT-3′ were used. The PCR products were cloned in front of the respective COOH termini as EcoRIClaI fragments, introducing an additional spacer of the two amino acids Ile/Asp after the HA tag.

For expression in LLC-PK1 cells or μ1A$^{-/-}$ fibroblasts stably transfected with mouse μ1B cDNA, the plasmids encoding the HA-tagged μ1A or μ1B were transfected using calcium phosphate precipitation as described previously (Fölsch et al., 1999; Meyer et al., 2000). Cells lines expressing wild-type (i.e., nontagged) μ1A or μ1B were as described previously (Fölsch et al., 1999).

Recombinant Adenoviruses and Antibodies

Defective recombinant adenoviruses encoding the low-density lipoprotein receptor (LDLR) (adLDLR), transferrin receptor (adTfnR), and FcLR(CT22) (adFcLR[CT22]) were as described previously (Fölsch et al., 1999).

Monoclonal anti-HA antibodies (clone 16B12) were purchased from BabCo. Specific anti-μ1B antibodies directed against the COOH terminus of μ1B were as described previously (Fölsch et al., 1999) and μ1A/B cross-reacting antibodies were the kind gift of Linton Traub (Washington University, St. Louis, MO). Polyclonal antibodies against GM130 (ML07) were obtained from Graham Warren (Yale University). Polyclonal antibodies against furin (PA1-062) were purchased from ABR. Monoclonal anti-γ-adaptin antibodies were purchased from Sigma-Aldrich (clone 100/3, for detection of γ-adaptin in LLC-PK1 cells) or Transduction Laboratories (clone 88, for detection of γ-adaptin in μ1A$^{-/-}$ fibroblasts). Polyclonal anti–γ-adaptin antibodies were the generous gift of Margaret Robinson (University of Cambridge, Cambridge, UK). Clone 100/3 was used for immunoprecipitations and Western blotting, the polyclonal anti–γ-adaptin antibody was used for immunofluorescence analysis in LLC-PK1 cells, and clone 88 was used for immunofluorescence analysis in μ1A$^{-/-}$ fibroblasts (Meyer et al., 2000). Monoclonal anticlathrin heavy chain antibodies (TD.1) were obtained from Pietro De Camilli (Yale University).

Hybridoma cell lines producing the monoclonal antibodies anti-LDLR (C7 for immunoprecipitations, 4A4 for Western blots) and anti-FcLR (2.4G2), were purchased from the American Type Culture Collection.

Secondary antibodies labeled with Alexa 488 or Alexa 594 and Texas red–labeled human transferrin (Tfn) were purchased from Molecular Probes.

Cell Culture

Stably transfected LLC-PK1 cells were maintained in α-MEM containing 10% (vol/vol) fetal bovine serum (FBS), 2 mM L-glutamine, and 1.8 mg/ml geneticin. μ1A$^{-/-}$ fibroblasts (Meyer et al., 2000) stably transfected with mouse μ1B cDNA or mouse μ1B cDNA and mouse μ1A-HA cDNA, were maintained in DME containing 10% (vol/vol) FBS, 2 mM L-glutamine, 200 μg/ml hygromycin or 200 μg/ml hygromycin, plus 200 μg/ml geneticin, respectively. All cell lines were incubated at 37°C in a 5% CO$_2$ incubator.

For immunofluorescence experiments, cells were seeded on Alcian blue–coated coverslips and cultured for 3–4 d. To allow for polarization, cells were plated on polycarbonate membrane filters at a density of 4 × 10^5 cells per 12-mm filter (0.4-μm pore size; Corning-Costar Transwell units) and cultured for 4–6 d with changes of medium in the basolateral chamber every day. If needed, cells were infected with defective adenoviruses (50–100 pfu/cell) as described previously (Fölsch et al., 1999).

Usually, the cells were fixed in 3% paraformaldehyde/PBS^{++} (PBS [2 g/liter KCl, 2 g/liter KH$_2$PO$_4$, 8 g/liter NaCL, 1.15 g/liter Na$_2$HPO$_4$, pH 7.4] plus 147 g/liter CaCl$_2$ × 2 H$_2$O, MgCl$_2$ × 6 H$_2$O) for 15 min; cell surface staining or total staining was performed as described previously (Fölsch et al., 1999). Permeabilization of the cells was achieved with the addition of 0.1% (filter-grown cells) or 0.2% (cells grown on coverslips) saponin (wt/vol) to the blocking and antibody solutions.

For double-labeling of HA-tagged μ1 with Tfn, cells seeded on coverslips were infected with a defective adenovirus (~100 pfu/cell) encoding human TfnR. 2 d after infection, cells were analyzed for Tfn uptake and subsequently stained with anti-HA antibodies. First, cells were starved in

---

[1]*Abbreviations used in this paper:* FSG; fish skin gelatin; HA, hemagglutinin; LDLR, low-density lipoprotein receptor; pfu, plaque forming unit; Tfn, transferrin; TfnR, Tfn receptor.

serum-free medium for 30 min at 37°C, then serum-free medium with TR-labeled Tfn (1:75) was added to allow for Tfn uptake for 30 min at 37°C. The cell surface was cleared by incubating the cells for an additional 2 min at room temperature in serum-free medium with an excess of unlabeled human Tfn (1 mg/ml). Cells were washed with ice-cold PBS^{++} and fixed in 3% paraformaldehyde for 15 min. The cells were permeabilized and labeled for immunofluorescence micrococopy as described above.

Filter-grown cells were analyzed using a ZEISS confocal microscope (Microsystem LSM) with an Axiovert 100 microscope and a ZEISS Plan-Neofluar 40× oil immersion objective. Preparations of cells grown on coverslips were analyzed using a ZEISS confocal microscope equipped with an Axiovert 100 microscope and a water immersion 63× objective (LSM 150 software; ZEISS). Images were enhanced and combined using Adobe Photoshop®.

Electron Microscopy and Immunocytochemistry Using Frozen Thin Sections

Cells were fixed for 2 d at 4°C with 4% paraformaldehyde (Electron Microscopy Sciences) in 0.25 M Hepes, pH 7.4, washed in PBS, scraped, and embedded in 10% gelatin. Small pieces of the gelatin pellets were infiltrated overnight at 4°C with 2.3 M sucrose in PBS, and then frozen in liquid nitrogen. Gold sections (95 nm thick) were cut using a Leica ultracut ultramicrotome with an FCS cryoattachment at −108°C and collected on formvar- and carbon-coated nickel grids using a 1:1 mixture of 2% methyl cellulose (25 centipoises; Sigma-Aldrich) and 2.3 M sucrose in PBS (Liou et al., 1996).

After quenching with 0.1 M NH$_4$Cl in PBS for 10 min, the grids were incubated for 20 min with a solution of 1% fish skin gelatin (FSG; Sigma-Aldrich) in PBS. They were then incubated with anti-HA antibodies (1:100 in PBS-FSG), washed four times for 4 min in PBS, incubated for 30 min at room temperature with rabbit anti–mouse IgGs (1:50 in PBS-FSG; Cappel/ICN Biomedicals), washed another four times for 4 min in PBS, and finally incubated for 30 min at room temperature with 5 nm protein A–gold (from the laboratory of J. Slot, University of Utrecht, Utrecht, the Netherlands) in PBS-FSG. After four final washes in PBS, the sections were fixed in 1% glutaraldehyde in PBS for 10 min, washed three times in water and stained for 10 min at room temperature with 2% neutral uranyl acetate (Electron Microscopy Sciences). After three short washes in water, the sections were infiltrated with a mixture of 1.8% methylcellulose and 0.5% uranyl acetate and air-dried.

Biochemical Procedures

Procedures such as preparing cells for Western blot analysis or immunoprecipitation experiments of radiolabeled samples were performed as described previously (Fölsch et al., 1999). HA-tagged µ1A was immunoprecipitated using the monoclonal anti-HA antibody 16B12, and HA-tagged µ1B by using the µ1B specific polyclonal antibody.

For cross-linking experiments, cells were split 1:1 into 6-well plates. 1 d after seeding, cells were infected with defective adenoviruses encoding wild-type or mutant LDLR as follows. Cells were washed once with serum-free medium and 100–200 pfu of the virus were added. After 1 h at 37°C, the cultures were fed with serum-containing medium and analyzed 21–22 h later. Cells were first washed once in ice-cold PBS^{++} and then incubated for 20 min at 4°C in glycerol buffer (10% glycerol, 0.1% saponin, 1 mM orthovanadate in PBS^{++}). Cells were washed once with this buffer and the cross-linking buffer was added (0.25 M sucrose, 1 mM orthovanadate in PBS^{++}). The cleavable cross-linker 3,3′-dithio-bis(sulfosuccinimidyl propionate) (DTSSP) was added from a freshly made 100× stock solution in DMSO to a final concentration of 100 µM. Cross-linking was allowed for 2 h at 4°C. After cross-linking, cells were washed once in PBS^{++}, and a buffer containing 100 mM glycine/pH 8.0 in PBS^{++} was added to stop the cross-linking reaction. After 20 min at 4°C, the cells were washed again in PBS^{++} and 1.25 ml lysis buffer (2.5% Triton X-100, 10 mM Tris-HCl, pH 7.4, 1× protease inhibitors [Boehringer] in PBS^{++}) was added to the samples. The cells were scraped with a cell scraper and passed four times through a 22.5-gauge needle and a 1-ml syringe. Lysis was completed for 30 min on ice followed by a clarifying spin (15 min at 13,000 rpm, Eppendorf centrifuge at 4°C). Cross-linking adducts were immunoprecipitated by incubating the lysis supernatant with anti-LDLR antibodies bound to protein G beads for 1.5 h end-over-end at 4°C. Immunoprecipitates were washed two times with lysis buffer containing 1% Triton X-100 and one time with lysis buffer without Triton X-100. The samples were resuspended in SDS sample buffer, vigorously shaken for 20 min at 4°C, boiled for 5 min, and analyzed by SDS-PAGE and Western blotting.

For coimmunoprecipitation experiments, the cells were treated exactly as for cross-linking experiments, but without the addition of a cross-linker.

Determination of protein concentration or detection of proteins after blotting onto nitrocellulose was performed using the BCA protein determination assay or the supersignal detection system, respectively, according to the supplier's instructions (Pierce Chemical Co.).

Results

HA-tagged µ1 Subunits Are Functionally Incorporated into AP-1 Complexes

In a previous study, we described two antipeptide antibodies that were specific for µ1B (Fölsch et al., 1999). Unfortunately, neither was suitable for immunofluorescence, a common problem with antibodies raised against the µ chains (Simpson et al., 1996; Dell'Angelica et al., 1999a,b). To establish the intracellular localization of µ1B-containing AP-1 complexes, we introduced internal HA tags into µ1A and µ1B between amino acids 230 and 231 (Fig. 1 A). These amino acids lie in a stretch of a weakly conserved region, presumably exposed at the surface of the protein by analogy to the crystal structure of µ2 (Owen and Evans, 1998). In addition, the corresponding site in µ2 did not prevent its incorporation into AP-2 complexes (Nesterov et al., 1999).

The cDNAs encoding the tagged proteins µ1A-HA and µ1B-HA were stably transfected into LLC-PK1 cells. First, cell lysates of parental and transfected LLC-PK1 cells were analyzed by Western blot. The transfected cell lines, LLC-PK1::µ1A-HA and LLC-PK1::µ1B-HA, were found to express similar amounts of the HA-tagged µ1 proteins when blotted with an anti-HA antibody (Fig. 1 B, anti-HA). In addition, both cell lines expressed slightly higher levels of γ-adaptin, one of the large 100-kD subunits of AP-1, than the parental LLC-PK1 cells (Fig. 1 B, anti–γ-adaptin). Decoration of the Western blot with an anti-µ1 antibody that detects both µ1A and µ1B revealed that µ1A-HA was present in great excess relative to its endogenous, untagged counterpart (Fig. 1 B, lanes 3 and 4). Indeed, the amount of endogenous µ1A appeared to have been decreased relative to untransfected parental cells (Fig. 1 B, lanes 1 and 2), suggesting that the excess HA-tagged µ1A competed with the untagged protein for assembly into AP-1 complexes. Unincorporated adaptor subunits are often degraded, perhaps accounting for the presumptive degradation product seen in Fig. 1 B (lane 4) (Zizioli et al., 1999; Meyer et al., 2000).

In contrast, endogenous µ1A expression in LLC-PK1::µ1B-HA cells was comparable to that found in the parental cells (Fig. 1 B, lanes 5 and 6). Yet again, presumptive degradation products were detected using the anti-µ1A/B antiserum, suggesting that not all of the transfected or endogenous proteins had been successfully incorporated into AP-1 complexes (Fig. 1 B, lane 6). These degradation products were not observed when untagged µ1A or µ1B were expressed in LLC-PK1 cells (Fölsch et al., 1999).

Next, we asked directly if the HA-tagged µ1 protein would incorporate into AP-1 complexes. For this purpose, LLC-PK1::µ1A-HA and LLC-PK1::µ1B-HA transfectants were metabolically labeled with [^{35}S]methionine/cysteine. Labeled cells were lysed and AP-1 was immunoprecipitated with anti–γ-adaptin antibodies. The labeled
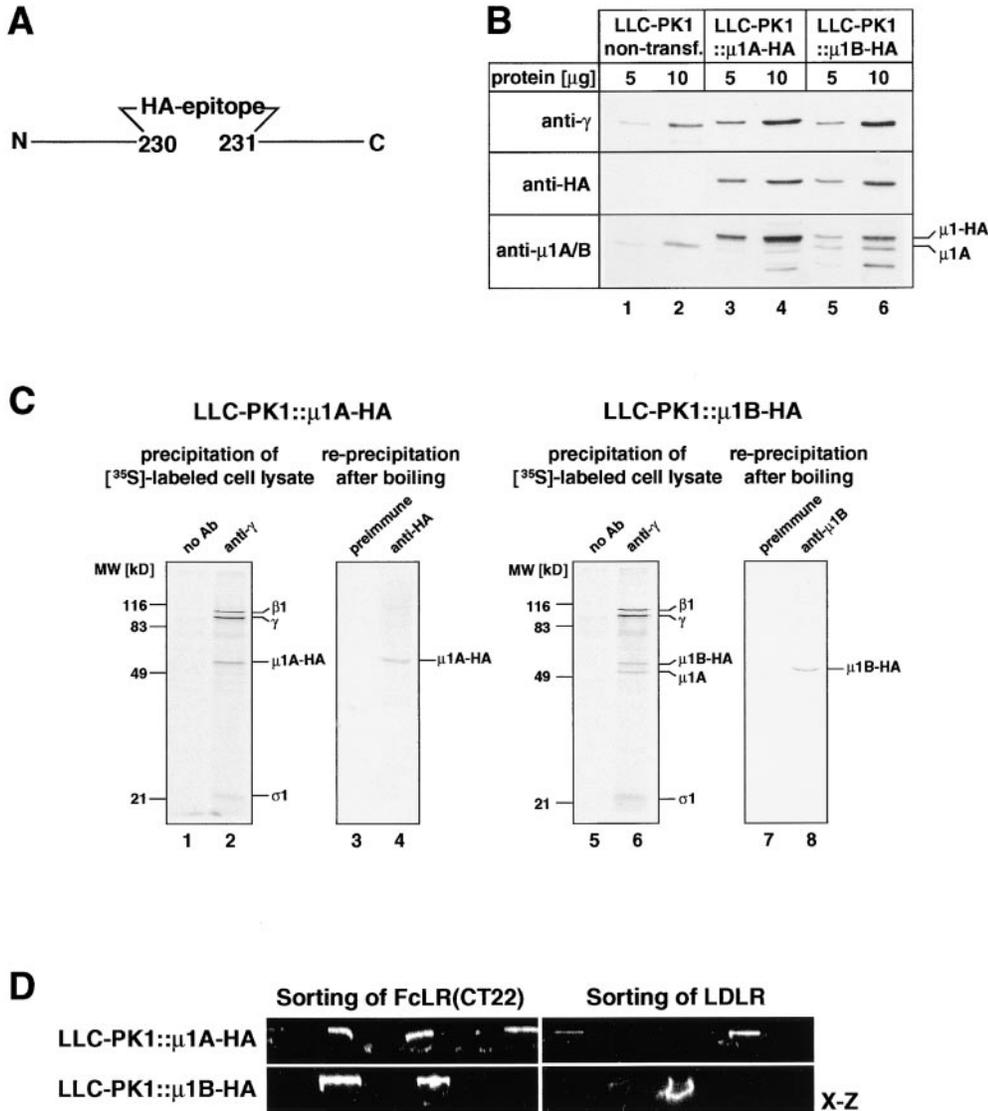
A

B

C

D

Figure 1. Expression and function of m1-HA. (A) Diagram showing the position of the internal HA-tag in μ1 protein (423 amino acids total). (B) Nontransfected LLC-PK1 cells, as well as LLC-PK1::μ1A-HA and LLC-PK1::μ1B-HA transfectants, were lysed in RIPA buffer and 5 and 10 μg of total protein were analyzed by Western blotting. γ-Adaptin, μ1-HA, and μ1 proteins were detected by immunodecoration with anti–γ-adaptin antibodies, anti-HA antibodies, and an antibody that cross-reacts with μ1A and μ1B, respectively. (C) LLC-PK1::μ1A-HA and LLC-PK1::μ1B-HA transfectants were metabolically labeled with [35S]methionine/cysteine overnight and lysed in Triton X-100 buffer. AP-1 complexes were immunoprecipitated using anti–γ-adaptin. The immunoprecipitates were boiled in SDS and one half of the extract was directly subjected to SDS-PAGE analysis. The remaining extract was diluted 20-fold in lysis buffer and μ1A-HA or μ1B-HA proteins were recaptured using anti-HA antibodies or specific anti-μ1B antibodies directed against the COOH terminus of μ1B, respectively. Immunoprecipitates were analyzed by SDS-PAGE and autoradiography. (D) LLC-PK1::μ1A-HA (top) and LLC-PK1::μ1B-HA (bottom) transfectants were grown on Transwell filters and infected with recombinant adenoviruses encoding the FcLR(CT22) chimera (left) or the LDLR (right). 2 d after the infection viable cells were incubated with antibodies directed against the ectodomain of FcLR or LDLR, respectively, fixed, and incubated with Alexa 488–labeled secondary antibodies as described in Material and Methods. Specimens were analyzed by confocal microscopy. Representative X–Z sections are shown.

bands that coimmunoprecipitated with γ-adaptin corresponded in molecular weight to β1-adaptin and σ1-adaptin, as well as μ1A-HA (Fig. 1 C, lane 2) or μ1A and μ1B-HA (Fig. 1 C, lane 6). To confirm the identities of μ1A-HA and μ1B-HA, the precipitates were boiled in SDS to disrupt the complex, the SDS was diluted with excess nonionic detergent, and the medium subunits were reprecipitated using anti-HA antibodies (μ1A-HA; Fig. 1 C, lane 4) or anti-μ1B antibodies (μ1B-HA; Fig. 1 C, lane 8). Thus, the transfected, epitope-tagged μ1 subunits appeared to assemble together with β-, γ-, and σ1-adaptins to form tagged AP-1A–HA or AP-1B–HA complexes.

Finally, we asked if HA-tagged μ1 would be functional in intact cells. For this purpose, polarized LLC-PK1 transfectants grown on filters were transfected with defective adenoviruses encoding either the LDLR or the apically targeted FcLR(CT22). The FcLR(CT22) is a chimera between the extracellular region and the membrane anchor of murine Fc receptor (FcRII) and the cytoplasmic tail of LDLR truncated at position 22. This truncation is known to remove all basolateral sorting information and the chimera is therefore sorted to the apical membrane of MDCK cells (Matter et al., 1994). 2 d after infection, the cells were analyzed by immunofluorescence using confocal microscopy for cell surface appearance of the receptors. As shown in the x/z-axis images in Fig. 1 D, expression of μ1B-HA but not of μ1A-HA restored basolateral localization of wild-type LDLR, indicating that the epitope-tagged μ1B could facilitate basolateral targeting in a fashion similar to that of the untagged protein (Fölsch et al., 1999). In contrast, FcLR(CT22) remained apically located in both μ1A-HA– and μ1B-HA–expressing cell lines.

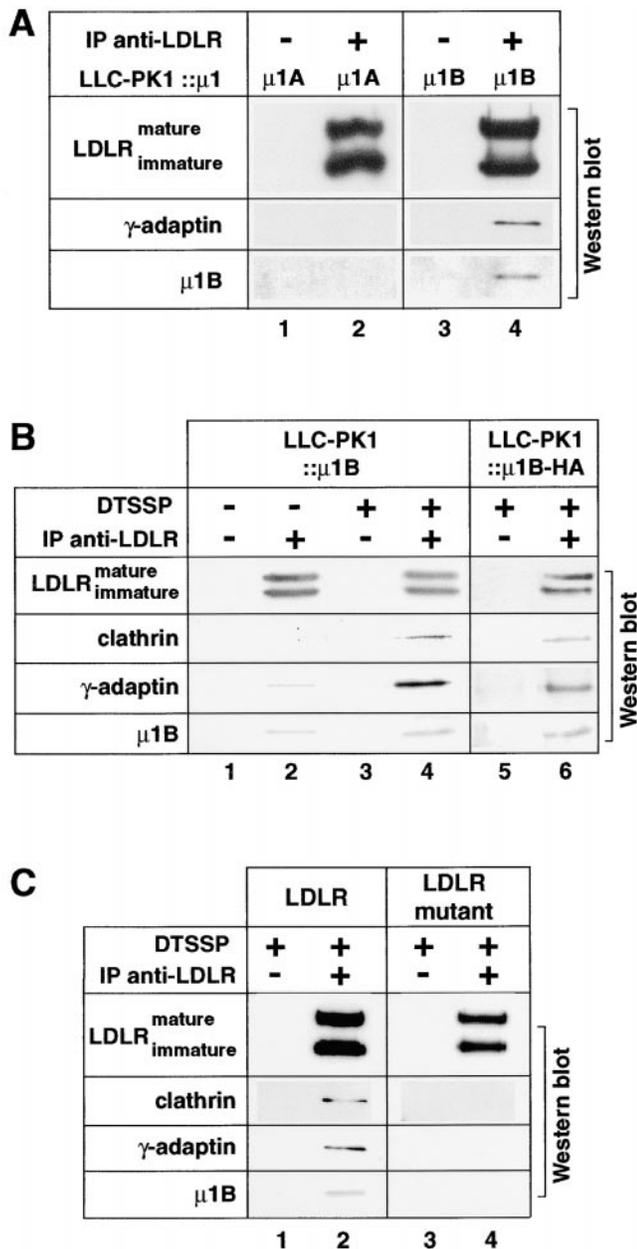In summary, we obtained stable LLC-PK1 cell lines expressing HA-tagged μ1A or μ1B subunits. Both μ1A-HA

Figure 2. AP-1B directly interacts with LDLR. (A) LLC-PK1::
μ1A or LLC-PK1::μ1B transfectants were infected with defective
adenoviruses encoding the LDLR. 1 d after the infections the cells
were lysed and the LDLR was immunoprecipitated (IP) with anti-
LDLR antibody (see Materials and Methods for details). Im-
munoprecipitates were analyzed by SDS-PAGE and Western
blotting. LDLR, γ-adaptin, and μ1B were detected by immuno-
decoration with anti-LDLR antibodies, anti–γ-adaptin antibodies,
or specific anti-μ1B antibodies raised against the COOH terminus
of μ1B, respectively. Samples representing equivalent amounts of
starting cell protein were added to each lane. (B) LLC-PK1 cells
transfected with μ1B (lanes 1–4) or μ1B-HA (lanes 5 and 6) were
infected with adLDLR. 1 d after infection the cells were incubated
with the cross-linker DTSSP (100 μM). After quenching, the cells
were lysed and the LDLR was immunoprecipitated as in A (de-
tails are described in Materials and Methods). Immunoprecipi-
tates were analyzed as described in A. Clathrin heavy chain was
detected by immunodecoration with anticlathrin heavy chain anti-
bodies. (C) LLC-PK1::μ1B transfectants were infected with
adLDLR (lanes 1 and 2) or adLDLR(Y18A/G34D) (lanes 3 and
4) and analyzed as described in B.

and μ1B-HA are incorporated into AP-1 complexes. Fur-
thermore, AP-1B–HA is active in mediating basolateral
targeting.

AP-1B Interacts with LDLR

The simplest explanation for how the AP-1B complex me-
diates basolateral targeting is that μ1B exerts an affinity
for basolateral targeting signals, thereby converting the
cargo specificity of AP-1 adaptors from endosome/lyso-
some-directed proteins to a subset of plasma membrane
proteins. Yet, basolateral targeting signals can be highly
divergent from signals for endosome/lysosome targeting,
whereas μ1A and μ1B are closely homologous. Thus, it is
not obvious that AP-1B complexes interact directly or in-
directly with basolateral cargo. To investigate the relation-
ship between AP-1B and LDLR, we performed a series of
coimmunoprecipitation and cross-linking experiments.

LLC-PK1 cells stably expressing μ1A or μ1B (Fölsch et
al., 1999) were infected with a defective adenovirus en-
coding LDLR. At times of maximal receptor expression
(∼21 h after infection), the infected cells were lysed in Tri-
ton X-100 and LDLR-immunoprecipitated. The precipi-
tates were then analyzed by Western blot to visualize the
LDLR and to determine if any AP-1B subunits were co-
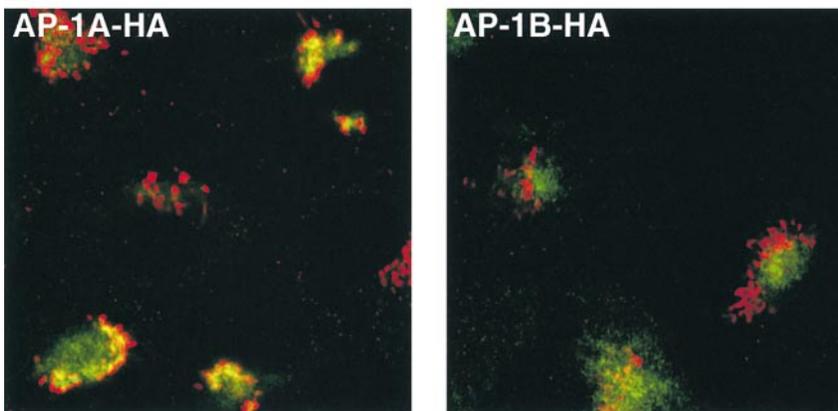precipitated.

As expected, the LDLR was detected as two bands, the
upper band representing the terminally glycosylated ma-
ture LDLR (160 kD) and the lower band corresponding to
the immature form of the receptor (140 kD) (Fig. 2 A). In
LLC-PK1 cells transfected with μ1A, no AP-1 was copre-
cipitated, as indicated by the absence of staining for
γ-adaptin (Fig. 2 A, lane 2); however, dependent on the
expression levels in the infected cells, a weak staining for
γ-adaptin could be observed (data not shown). Thus, AP-
1A interacts only weakly with the LDLR. In LLC-PK1::
μ1B transfectants, however, substantially more AP-1
(γ-adaptin) was brought down with anti-LDLR antibodies
(Fig. 2 A, compare γ-adaptin bands in lanes 2 and 4). Most
importantly, μ1B was also coprecipitated.

To further characterize the interaction between AP-1B
and LDLR, we performed chemical cross-linking using the
cleavable cross-linker DTSSP. As shown in Fig. 2 B, addi-
tion of DTSSP greatly enhanced the amount of γ-adaptin
coprecipitated with the anti-LDLR antibodies and mod-
estly enhanced coprecipitation of μ1B. This suggests, as
expected, that the cross-linking would occur predomi-
nantly between LDLR and the large subunits of the adap-
tor complex, rather than between the LDLR and the
potentially interacting μ1B subunit. Upon cell lysis, com-
plexes between LDLR and AP-1, as well as AP-1 com-
plexes themselves, may dissociate and therefore we ob-
serve an enhancement of γ-adaptin only and not of μ1B in
the immunoprecipitates after cross-linking. Similar results
were obtained for cells stably transfected with μ1B or the
epitope-tagged μ1B-HA construct (Fig. 2 B).

In addition to AP-1B subunits, we observed cross-link
products between LDLR and clathrin (Fig. 2 B, lanes 4
and 6), suggesting that clathrin is involved in the formation
of AP-1B–containing vesicles. Under the same conditions,
no cross-link products to AP-2 were observed (data not
shown). However, cross-linking to clathrin was observed
when LLC-PK1::μ1B-HA transfectants were used, con-

A μ1-HA | γ-adaptin (AP-1 complex) | merge

AP-1A-HA

AP-1B-HA
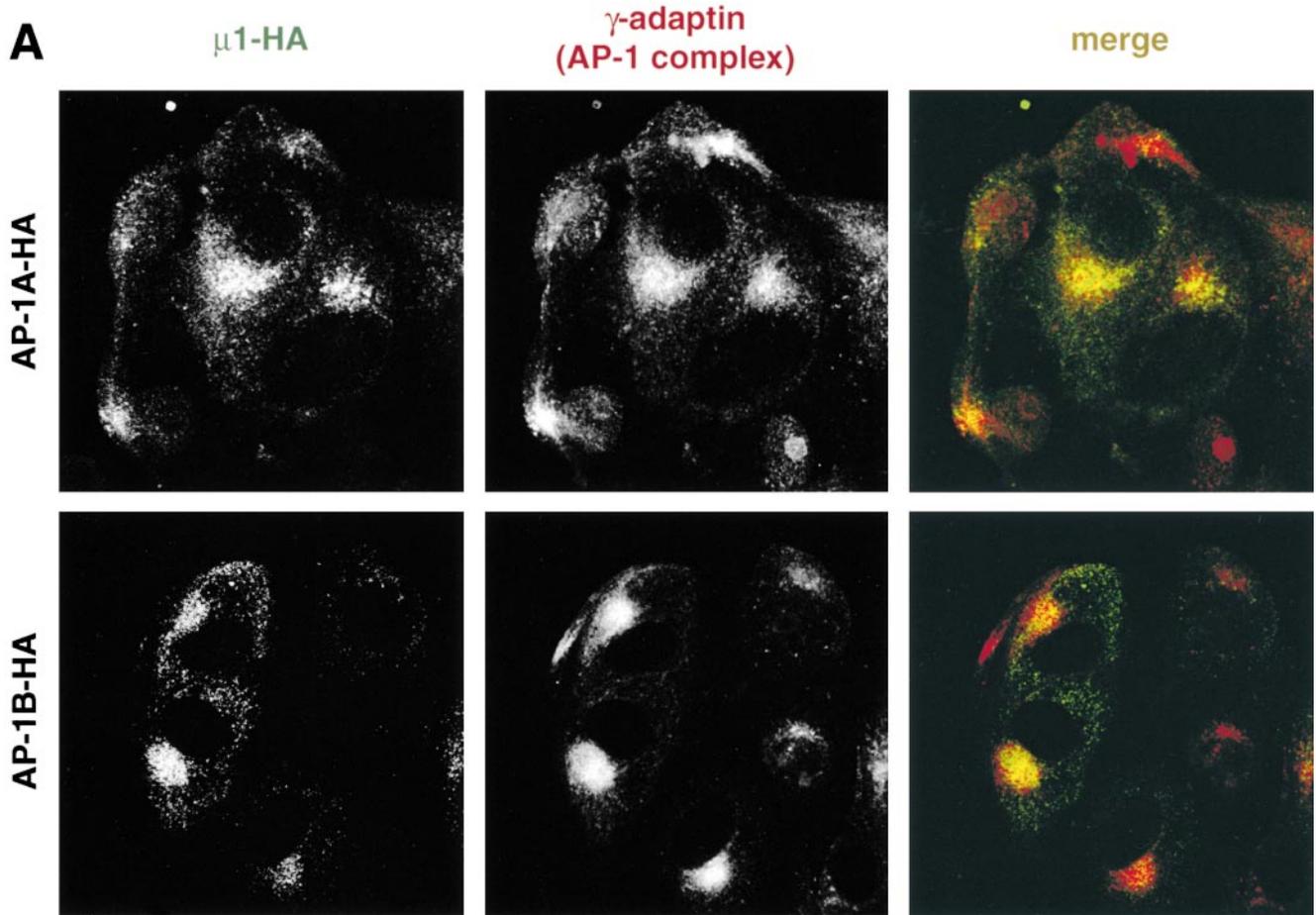
B μ1-HA and GM130 (cis-Golgi)

AP-1A-HA | AP-1B-HA

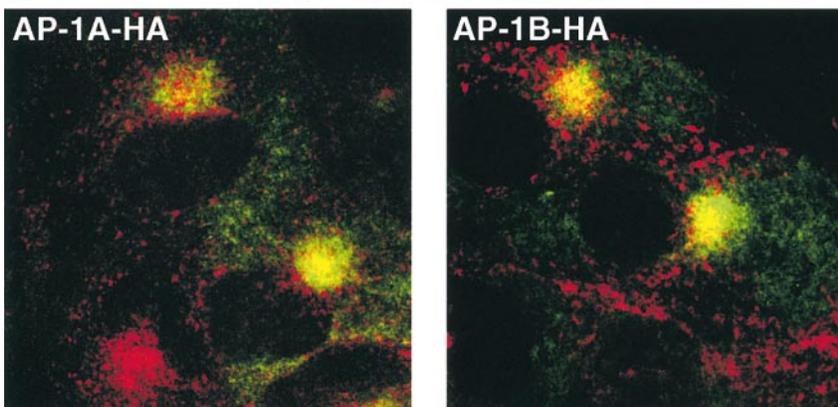**C** μ1-HA and Tfn (early and recycling endosomes)

AP-1A-HA | AP-1B-HA

Figure 3. AP-1–HA localizes to a perinuclear region. LLC-PK1::μ1A-HA transfectants (A–C, top) and LLC-PK1 cells transfected with μ1B-HA (bottom) were fixed and incubated with anti-HA antibodies (A, left) in combination with (A) anti–γ-adaptin antibodies (middle), (B) anti-GM130 antibodies, or (C) Texas red–labeled Tfn. These incubations were followed by an incubation with Alexa 488–labeled (anti-HA staining) and Alexa 594–labeled (anti–γ-adaptin and anti-GM130 staining) secondary antibodies. Specimens were analyzed by confocal microscopy and representative images are shown.
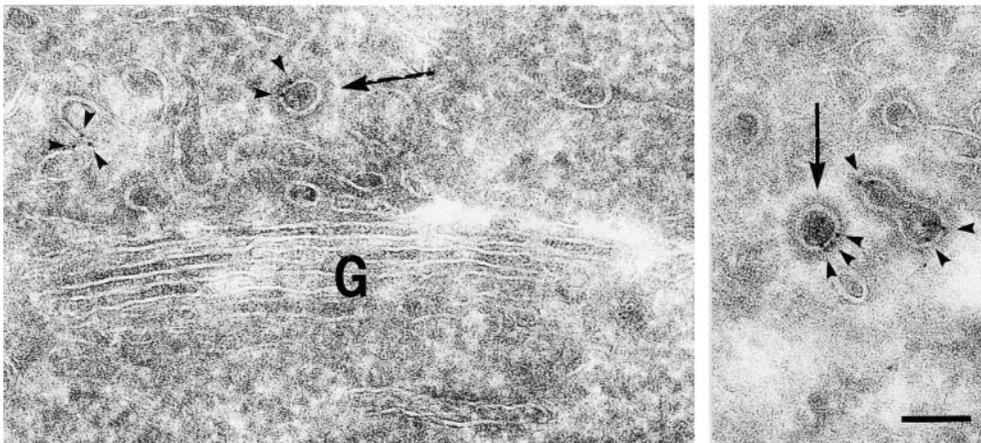
A AP-1A-HA
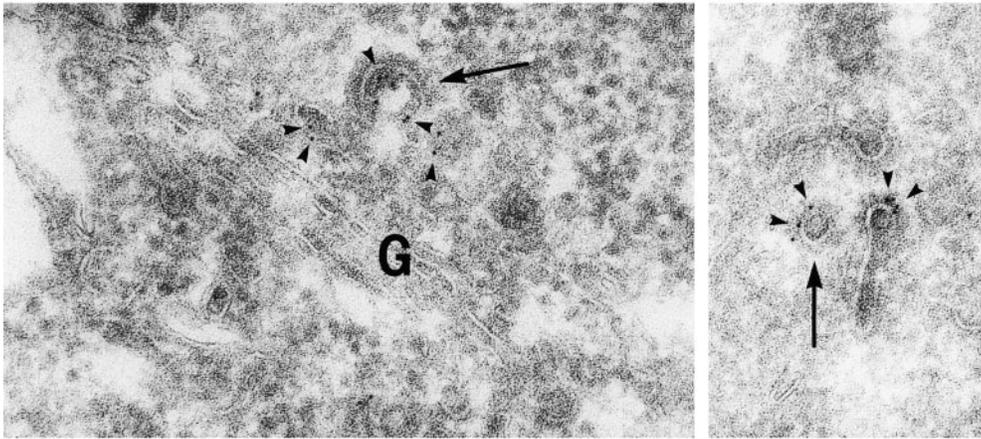
B AP-1B-HA

Figure 4. AP-1–HA is found on clathrin-coated structures. LLC-PK1::μ1A-HA (A) or LLC-PK1::μ1B-HA transfectants (B) were analyzed by immunoelectron microscopy (see Materials and Methods for details). HA-tagged μ1 proteins were visualized using anti-HA antibodies, followed by incubations with anti–mouse IgG antibodies and protein A–gold. Arrowheads highlight gold particles and arrows denote clathrin-coated structures. Bar, 100 nm.

firming that complexes containing μ1B-HA behaved similarly to those containing the untagged μ1B.

We next tested if the interaction between LDLR and AP-1B was dependent on either of the LDLR's two tyrosine-based sorting signals. LLC-PK1::μ1B transfectants were infected with an adenovirus encoding a mutant form of LDLR (Y18A/G34D) in which the tyrosine at position 18 was changed to an alanine and the glycine residue at position 34 was changed to a glutamic acid. Thus, both the "proximal" and "distal" basolateral targeting signals were disrupted, resulting in a receptor that was largely expressed at the apical surface of MDCK cells and even μ1B-transfected LLC-PK1 cells (Matter et al., 1994; Koivisto, U.-M., and I. Mellman, manuscript in preparation; H. Fölsch and Mellman, I., unpublished observations). Neither AP-1B nor clathrin could be cross-linked to the mutant LDLR, indicating that AP-1B specifically interacts with its basolateral sorting signals (Fig. 2 C, lane 4).

Taken together, these results suggest that AP-1B mediates basolateral targeting by directly interacting with the basolateral targeting motifs of cargo molecules, and also that clathrin is involved in the formation of transport vesicles targeted to the basolateral plasma membrane.

AP-1B Complexes Localize to a Perinuclear Region Adjacent to the Golgi Complex

Having demonstrated that μ1B-HA behaves functionally like the nontagged protein, we next used the μ1A-HA–

and μ1B-HA–transfected cell lines to determine their intracellular distribution. Cells grown on coverslips were double-labeled with anti-HA antibodies to visualize the AP-1A–HA or AP-1B–HA complexes (green) together with antibodies against various endogenous marker proteins (red) and analyzed using confocal microscopy.

Labeling with anti-HA antibodies produced perinuclear staining patterns in both AP-1A–HA– and AP-1B–HA–expressing cell lines (Fig. 3 A, left). As shown in Fig. 3, both μ1A-HA (top) and μ1B-HA (bottom) exhibited good regional colocalization with γ-adaptin. However, the extent of colocalization was not complete, with some μ1 labeling found in the periphery, particularly in the case of μ1B. This might simply reflect different sensitivities of the HA and γ-adaptin antibodies used, relative accessibility of the epitopes, or possibly a somewhat differential distribution of AP-1A and AP-1B complexes.

Next, we performed double labeling of AP-1–HA and GM130, a structural protein of cisternal elements of the Golgi complex (Nakamura et al., 1995). GM130 antibodies showed characteristic perinuclear staining (Fig. 3 B, red). As might be expected for TGN markers, the AP-1 complexes localized to one side of the Golgi complex, adjacent to but distinct from the GM130-positive structures.

To determine if any AP-1A or AP-1B complexes were associated with endosomes, stable transfectants were grown on coverslips and infected with a defective adenovirus encoding the human TfnR. 2 d after infection, the cells
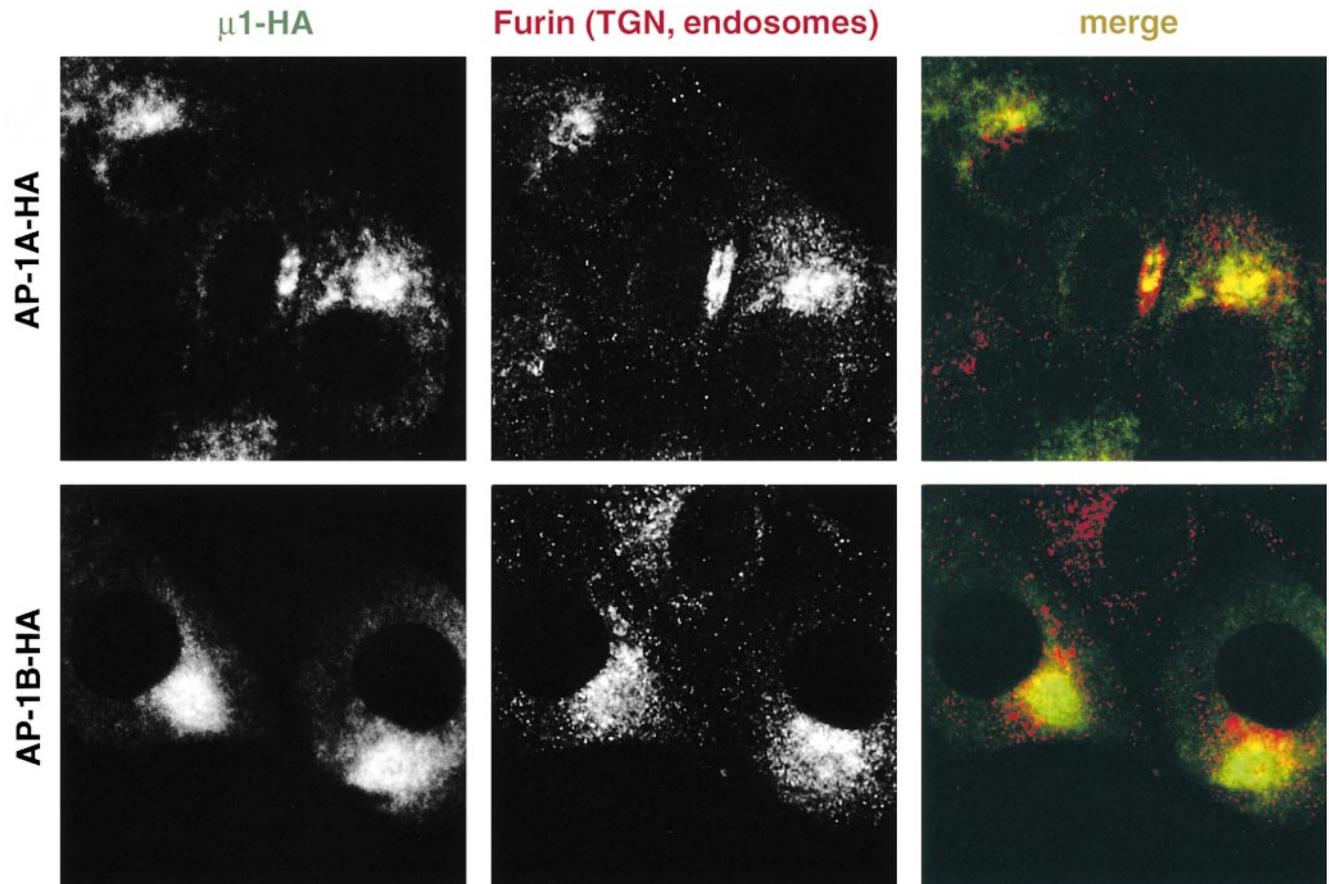
Figure 5. AP-1A–HA, but not AP-1B-HA, colocalizes with furin. LLC-PK1 cells transfected with μ1A-HA (top) or μ1B-HA (bottom) were double-labeled with anti-HA antibodies (left) and antifurin antibodies (middle) in combination with Alexa 488–labeled (anti-HA staining) and Alexa 594–labeled (antifurin staining) secondary antibodies. Specimens were analyzed by confocal microscopy. Representative images are shown (merged images are shown on right).

were incubated with Texas red–labeled Tfn for 30 min at 37°C under conditions that would stain the entire early endosome/recycling endosome pathway (Sheff et al., 1999). Early endosomes are punctate structures throughout the cell, whereas the recycling endosomes are generally clustered in a perinuclear region (Fig. 3 C, red). Although some AP-1A–HA and AP-1B–HA colocalized regionally with Texas red–labeled Tfn, it was evident that AP-1 and recycling endosomes did not colocalize completely in perinuclear and especially in peripheral early endosome–containing regions of the cytoplasm. This is consistent with previously reported localizations of AP-1, in which some localization to endosomes has been observed (Futter et al., 1998). Thus, both AP-1A and AP-1B may be similarly distributed with respect to the more perinuclear recycling endosomes.

AP-1B Is Found Associated with Clathrin-coated Buds of the TGN

To further characterize the intracellular localization of AP-1B, we performed immunoelectron microscopy on frozen sections of LLC-PK1::μ1A-HA or LLC-PK1:: μ1B-HA transfectants. Most of the labeling for both AP-1A–HA (Fig. 4 A) and AP-1B–HA (Fig. 4 B) complexes with protein A–gold (arrowheads) was associated with buds, vesicles, and tubules on one side of the Golgi stack. This side of the stack was also characterized by morpho-

logically identifiable clathrin coats, strongly suggesting that it corresponds to the trans side. Indeed, and as expected from previous work for untagged AP-1A complexes, many of the gold particles were associated with clathrin coats (denoted by arrows) (Hirst and Robinson, 1998). We conclude that, like AP-1A and AP-1B, complexes can associate with clathrin coats in the TGN, suggesting that their function is associated with clathrin assembly. Often, apparently free-coated vesicles seemed to be more heavily stained for either μ1A or μ1B than were the clathrin-coated tubules that emerged from the TGN. This might reflect either the relative densities or accessibilities of the μ1 or the epitope tags at different stages of coat assembly.

AP-1A and AP-1B May Localize to Different Regions of the TGN

We next attempted to assess the distributions of AP-1A and AP-1B relative to each other. Since we were unable to generate cell lines that expressed differentially tagged μ1 chains, we examined their distribution in single transfectants relative to a common endogenous marker. For this purpose we used furin, a proprotein convertase that recycles between the TGN and endosomes. Furin has been shown to interact with AP-1A through the adaptor protein PACS-1 during retrieval of furin from endosomes to the TGN and is thought to interact directly with AP-1A dur-
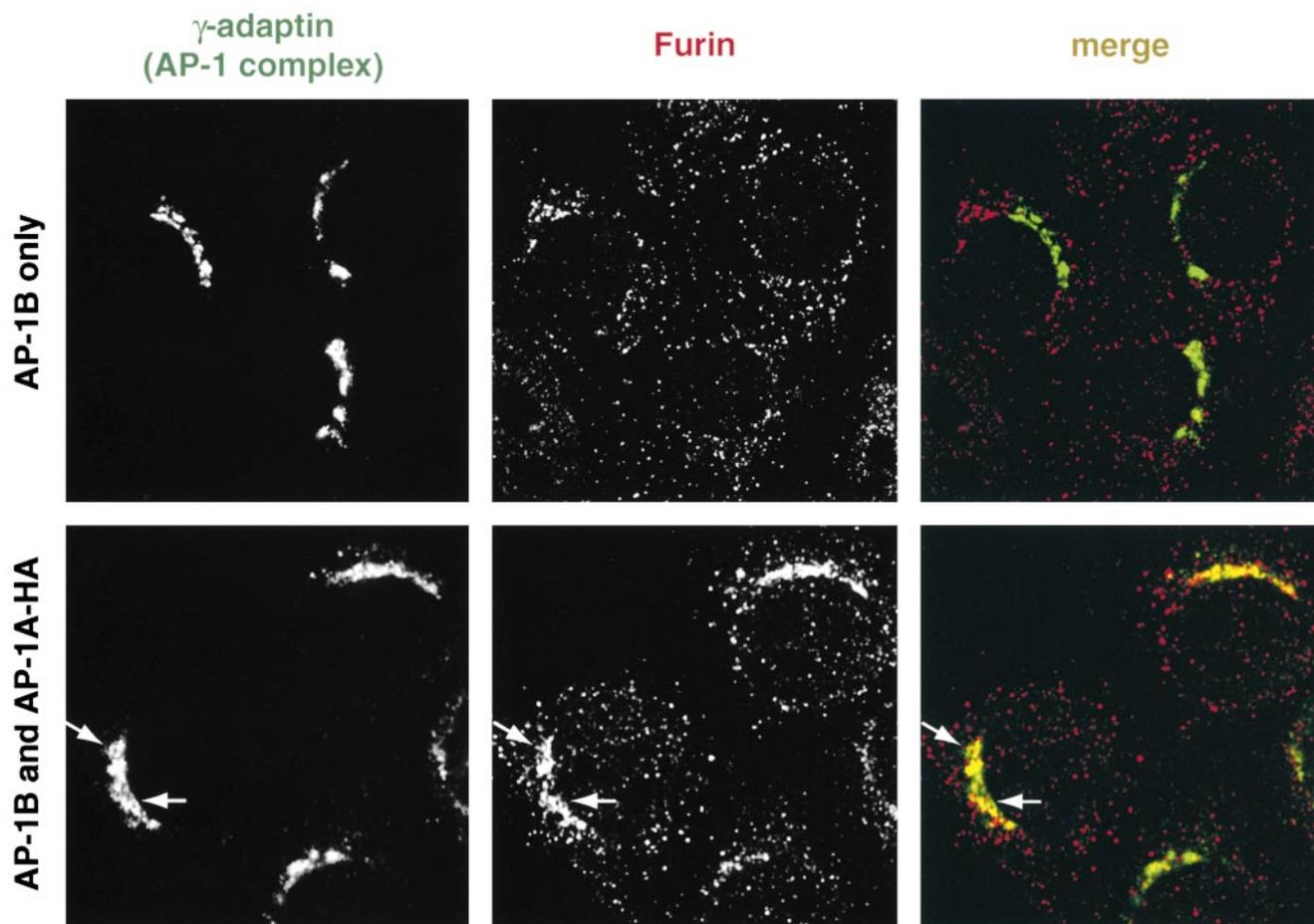
Figure 6. AP-1A is necessary for furin localization at the TGN. $\mu 1A^{-/-}$ fibroblasts stably transfected with $\mu 1B$ alone (top) or with $\mu 1B$ and $\mu 1A$-HA (bottom) were double-labeled with anti–γ-adaptin antibodies (left) and antifurin antibodies (middle) in combination with Alexa 488–labeled (anti-γ staining) and Alexa 594–labeled (antifurin staining) secondary antibodies. Specimens were analyzed by confocal microscopy and representative images are shown. The arrows denote regions in the AP-1B/AP-1A–HA transfectants that are positive for AP-1 but negative for furin.

ing transfer from the TGN to the endosomes (Molloy et al., 1999; Teuchert et al., 1999). Thus, furin should colocalize, at least in part, with AP-1 in the TGN.

As shown in Fig. 5, AP-1A–HA and furin exhibited overlapping, albeit somewhat distinct, distributions, suggesting that they were at least partly localized to the same regions of the TGN and/or endosomes (top). In contrast, the staining pattern of AP-1B–HA was almost entirely different from that of furin (Fig. 5, bottom).

Although we have yet to achieve furin staining at the electron microscopic level, these results suggest that AP-1A and AP-1B may define at least partially distinct subdomains of the TGN and/or endosomes. In any event, given that AP-1A–HA and AP-1B–HA exhibited distributions relative to furin that were distinct, it is apparent that the two adapter complexes do not share identical distributions. This situation may reflect differences in cargo specificity of the AP-1A and AP-1B complexes.

TGN Localization of Furin Is Dependent on m1A Expression

Recently, Meyer et al. (2000) generated a cell line of mouse embryonic fibroblasts that were deficient in $\mu 1A$ ($\mu 1A^{-/-}$ fibroblasts) and exhibited a loss of perinuclear

γ-adaptin staining. The diffuse γ-adaptin staining observed in these cells could be rescued by stably transfecting the cells with untagged mouse $\mu 1B$ cDNA (Schu, P., unpublished observations; Fig. 6), suggesting that $\mu 1B$ could substitute for $\mu 1A$ in recruiting the other three AP-1 subunits to the TGN. Therefore, we tested whether $\mu 1B$ expression in the absence of $\mu 1A$ would also affect the distribution of furin, which, based on our localization experiments (Fig. 5), would appear to be more likely to interact with AP-1A than with AP-1B.

$\mu 1A^{-/-}$ fibroblasts stably transfected with $\mu 1B$, with or without cotransfected $\mu 1A$, were thus labeled with antibodies against γ-adaptin (as a marker for assembled AP-1B complexes) and furin. As shown in Fig. 6 (top), there was virtually no overlap between AP-1B and furin in the absence of AP-1A. In fact, furin was no longer even localized to the TGN region, but rather was found associated with punctate structures, possibly endosomes, that were devoid of γ-adaptin (i.e., AP-1B) staining. Thus, normal localization of furin to the TGN does not occur when only AP-1B is expressed.

However, the furin phenotype could be reversed by expressing $\mu 1A$-HA in the $\mu 1A^{-/-}$, $\mu 1B^+$ fibroblasts (Fig. 6, bottom). Fibroblasts expressing AP-1A–HA in addition to AP-1B showed a more typical perinuclear staining pattern

for furin. Indeed, furin now colocalized extensively with γ-adaptin in the perinuclear region. Given the inability of μ1B alone to complement the ectopic distribution of furin in μ1A$^{-/-}$ cells, the coordinate distribution of furin and γ-adaptin seemed likely to reflect furin's colocalization with AP-1A rather than AP-1B. Indeed, we often noted many regions of the TGN that were stained only for γ-adaptin and not for furin in cells expressing both AP-1A and -1B (Fig. 6, bottom, arrows). Conceivably, these areas represented regions of the TGN which were enriched in AP-1B relative to AP-1A. Double-labeling of these cells with antibodies against furin and μ1A-HA revealed complete colocalization of furin and AP-1A–HA (data not shown).

Taken together, the strict dependence of furin on AP-1A for its intracellular distribution may suggest that AP-1A and AP-1B may not only localize to different subdomains in the TGN, but that this different localization reflects their involvement in different pathways from the TGN to endosomes/lysosomes or the basolateral plasma membrane, respectively.

Discussion

We have addressed two questions critical for understanding how AP-1B mediates basolateral targeting in polarized epithelial cells. First, we provided biochemical evidence to support the likelihood that μ1B directly recognizes basolateral targeting signals on membrane proteins such as LDLR. This was a critical unknown given that a previous yeast two-hybrid assay suggested that the sequences recognized by μ1B represented a subset of the canonical YXXΦ motif (Ohno et al., 1999). Although the LDLR contains two basolateral determinants that are tyrosine dependent, neither conforms to this motif (Matter et al., 1992). We have shown that wild-type LDLR physically interacts with AP-1B, but not AP-1A, both by coprecipitation with and without the use of a chemical cross-linking agent. Moreover, the interaction was greatly reduced by point mutations affecting critical residues required for efficient basolateral targeting. Thus, the AP-1B complex specifically binds to either or both basolateral targeting signals found on LDLR and presumably other basolateral plasma membrane proteins. It is also clear that this interaction is due to the presence of the μ1B subunit in the complex, further suggesting that it is this subunit which binds directly to the basolateral targeting signal. If so, one might imagine that μ1B may interact with these signals in a fashion somewhat dissimilar to that inferred from the structure of μ2 interaction with clathrin-coated pit signals (Owen and Evans, 1998). Alternatively, we cannot yet exclude that the interaction between LDLR and μ1B is facilitated by an additional as yet unidentified adaptor protein (Wan et al., 1998).

Whatever the precise nature of the interaction, it appears likely that AP-1B acts to facilitate cargo selection into nascent basolateral vesicles which are also invested by a clathrin coat. Since we could visualize μ1B associated with clathrin-coated buds that were connected to the TGN, we suspect that an interaction between newly synthesized basolateral proteins and AP-1B occurs upon exit from the Golgi complex. That the TGN serves as the primary site for sorting of apical and basolateral proteins in many types of epithelial cells has been long known (Keller and Simons, 1997), but a role for clathrin in this process

has not before been established. Indeed, clathrin has for years been thought to play no role in biosynthetic membrane traffic to the plasma membrane, based on its apparent failure to associate with vesicular stomatitis virus G protein accumulated in the TGN of fibroblasts at 20°C (Griffiths et al., 1985). However, these classical experiments were conducted in cells expected to be negative for μ1B; μ1A-containing clathrin buds, based on the evidence shown here, would not be expected to accumulate vesicular stomatitis virus G protein, despite the fact that it has a basolateral targeting signal. In this respect, it is interesting to note that at least one other basolateral protein, polymeric immunoglobulin receptor, has been reported to coimmunoprecipitate with γ-adaptin after accumulation in the TGN (Orzech et al., 1999), although this association was not demonstrated to be AP-1B specific.

Our results are also consistent with the localization of at least some AP-1B to endosomes. This would be in accord with previous work showing that clathrin coats, together with the AP-1 subunit γ-adaptin, can be found on TfnR-positive endosome populations, especially in polarized MDCK cells (Stoorvogel et al., 1996; Futter et al., 1998). Endosomes in epithelial cells are capable of decoding the same signals for polarized transport as is the TGN, a feature which ensures the maintenance of polarity despite continued endocytosis and recycling (Matter et al., 1993; Aroeti and Mostov, 1994). It would appear that this in fact might be a clathrin-dependent process, as suggested earlier (Futter et al., 1998). Additional mechanisms may yet be discovered as it is the case that endosomes in hepatocytes mediate basolateral sorting, despite the fact that these cells appear not to express μ1B (Ohno et al., 1999).

Although electron microscopy failed to indicate any obvious differences in the overall organization of the Golgi complex in cells that do or do not express AP-1B, the degree to which AP-1B and AP-1A appeared to define distinct intracellular domains was striking. Although it has not yet been possible to localize the two adaptor complexes relative to each other directly, at the level of immunofluorescence they did exhibit different patterns relative to the TGN marker furin. AP-1A staining showed significant colocalization with furin, whereas AP-1B did not. In addition, in fibroblasts expressing AP-1B as the only AP-1 complex, TGN staining of furin was lost but could be restored by exogenously expression of μ1A. This is perhaps not surprising, since the budding of furin-containing vesicles from the TGN is mediated by AP-1A. Furin transport from endosomes also involves AP-1A, albeit in association with the coadaptor PACS-1 (Wan et al., 1998; Molloy et al., 1999). The fact that AP-1B staining showed little, if any, overlap with furin is remarkable given the high degree of structural relatedness between the AP-1A and AP-1B complexes. This result emphasizes the importance of the μ subunits in determining not only the functional specificity, but even the intracellular localization of a given adaptor complex. The two complexes clearly mediate different functions, as AP-1A will not substitute for AP-1B in basolateral transport nor will AP-1B substitute for AP-1A in at least retrieval of furin back to the TGN.

Conceivably, cargo selection by AP-1 adaptors and adaptor recruitment to membranes are closely linked events. Indeed, there is evidence that the recruitment of AP-1A onto TGN membranes may be dependent both on the presence

of activated ARF-1 and AP-1A cargo molecules (Le Borgne et al., 1996; Le Borgne and Hoflack, 1997), although this point remains controversial (Zhu et al., 1999). If cargo proteins did participate in coat recruitment, the expression of μ1B might itself help generate a TGN subdomain, in which nascent basolateral proteins become concentrated. Alternatively, such subdomains might preexist, perhaps by the selective localization of a putative "docking protein" that first binds AP-1B to the membrane, which in turn concentrates basolateral cargo such as LDLR. It is interesting that the TGN has already been observed to exhibit morphologically distinct subdomains with clathrin-coated and nonclathrin-coated vesicles budding from physically different regions (Ladinsky et al., 1994, 1999). Sorting of basolateral membrane proteins, be they cargo or docking proteins, into different areas of the TGN would have as a precedent the lateral segregation of recycling receptors and related molecules into tubular elements of endosomes (Geuze et al., 1987, 1988; Sönnichsen et al., 2000).

It seems that the fate of a TGN-derived coated vesicle is most likely to depend on the predominant adaptor complex it contains. Targeting molecules (SNAREs, Rabs) might be recruited by direct or indirect interactions with adaptor complexes. In this respect it is interesting to note that the v-SNARE VAMP-7 has a potential adaptor complex binding motif in its cytoplasmic domain (Advani et al., 1999). Thus, AP-1B may directly determine the fate of the vesicles it helps to form by specifying the inclusion of those proteins needed for targeting and fusion at the basolateral plasma membrane.

References

Advani, R.J., B. Yang, R. Prekeris, K.C. Lee, J. Klumperman, and R.H. Scheller. 1999. VAMP-7 mediates vesicular transport from endosomes to lysosomes. *J. Cell Biol.* 146:765–776.

Aroeti, B., and K.E. Mostov. 1994. Polarized sorting of the polymeric immunoglobulin receptor in the exocytotic and endocytotic pathways is controlled by the same amino acids. *EMBO (Eur. Mol. Biol. Organ.) J.* 13:2297–2304.

Bonifacino, J.S., and E.C. Dell'Angelica. 1999. Molecular bases for the recognition of tyrosine-based sorting signals. *J. Cell Biol.* 145:923–926.

Cohen, A.R., D.F. Woods, S.M. Marfatia, Z. Walther, A.H. Chishti, J.M. Anderson, and D.F. Woods. 1998. Human CASK/LIN-2 binds syndecan-2 and protein 4.1 and localizes to the basolateral membrane of epithelial cells. *J. Cell Biol.* 142:129–138.

Dell'Angelica, E.C., J. Klumperman, W. Stoorvogel, and J.S. Bonifacino. 1998. Association of the AP-3 adaptor complex with clathrin. *Science.* 280:431–

434.

Dell'Angelica, E.C., C. Mullins, and J.S. Bonifacino. 1999a. AP-4, a novel protein complex related to clathrin adaptors. *J. Biol. Chem.* 274:7278–7285.

Dell'Angelica, E.C., V. Shotelersuk, R.C. Aguilar, W.A. Gahl, and J.S. Bonifacino. 1999b. Altered trafficking of lysosomal proteins in Hermansky-Pudlak syndrome due to mutations in the β3A subunit of the AP-3 adaptor. *Mol. Cell.* 3:11–21.

Drake, M.T., Y. Zhu, and S. Kornfeld. 2000. The assembly of AP-3 adaptor complex-containing clathrin-coated vesicles on synthetic liposomes. *Mol. Biol. Cell.* 11:3723–3736.

Drubin, D.G., and W.J. Nelson. 1996. Origins of cell polarity. *Cell.* 84:335–344.

Fölsch, H., H. Ohno, J.S. Bonifacino, and I. Mellman. 1999. A novel clathrin adaptor complex mediates basolateral targeting in polarized epithelial cells. *Cell.* 99:189–198.

Futter, C.E., A. Gibson, E.H. Allchin, S. Maxwell, L.J. Ruddock, G. Odorizzi, D. Domingo, I.S. Trowbridge, and C.R. Hopkins. 1998. In polarized MDCK cells basolateral vesicles arise from clathrin-γ-adaptin–coated domains on endosomal tubules. *J. Cell Biol.* 141:611–623.

Geuze, H.J., J.W. Slot, and A.L. Schwartz. 1987. Membranes of sorting organelles display lateral heterogeneity in receptor distribution. *J. Cell Biol.* 104:1715–1723.

Geuze, H.J., W. Stoorvogel, G.J. Strous, J.W. Slot, J.E. Bleekemolen, and I. Mellman. 1988. Sorting of mannose 6-phosphate receptors and lysosomal membrane proteins in endocytic vesicles. *J. Cell Biol.* 107:2491–2501.

Griffiths, G., S. Pfeiffer, K. Simons, and K. Matlin. 1985. Exit of newly synthesized membrane proteins from the trans cisterna of the Golgi complex to the plasma membrane. *J. Cell Biol.* 101:949–964.

Hirst, J., and M.S. Robinson. 1998. Clathrin and adaptors. *Biochim. Biophys. Acta.* 1404:173–193.

Hirst, J., N.A. Bright, B. Rous, and M.S. Robinson. 1999. Characterization of a fourth adaptor-related protein complex. *Mol. Biol. Cell.* 10:2787–2802.

Keller, P., and K. Simons. 1997. Post-Golgi biosynthetic trafficking. *J. Cell Sci.* 110:3001–3009.

Ladinsky, M.S., J.R. Kremer, P.S. Furcinitti, J.R. McIntosh, and K.E. Howell. 1994. HVEM tomography of the trans-Golgi network: structural insights and identification of a lace-like vesicle coat. *J. Cell Biol.* 127:29–38.

Ladinsky, M.S., D.N. Mastronarde, J.R. McIntosh, K.E. Howell, and L.A. Staehelin. 1999. Golgi structure in three dimensions: functional insights from the normal rat kidney cell. *J. Cell Biol.* 144:1135–1149.

Le Borgne, R., and B. Hoflack. 1997. Mannose 6-phosphate receptors regulate the formation of clathrin-coated vesicles in the TGN. *J. Cell Biol.* 137:335–345.

Le Borgne, R., G. Griffiths, and B. Hoflack. 1996. Mannose 6-phosphate receptors and ADP-ribosylation factors cooperate for high affinity interaction of the AP-1 Golgi assembly proteins with membranes. *J. Biol. Chem.* 271:2162–2170.

Liou, W., H.J. Geuze, and J.W. Slot. 1996. Improving structural integrity of cryosections for immunogold labeling. *Histochem. Cell Biol.* 106:41–58.

Matter, K. 2000. Epithelial polarity: sorting out the sorters. *Curr. Biol.* 10:R39–R42.

Matter, K., and I. Mellman. 1994. Mechanisms of cell polarity: sorting and transport in epithelial cells. *Curr. Opin. Cell Biol.* 6:545–554.

Matter, K., W. Hunziker, and I. Mellman. 1992. Basolateral sorting of LDL receptor in MDCK cells: the cytoplasmic domain contains two tyrosine-dependent targeting determinants. *Cell.* 71:741–753.

Matter, K., J.A. Whitney, E.M. Yamamoto, and I. Mellman. 1993. Common signals control low density lipoprotein receptor sorting in endosomes and the Golgi complex of MDCK cells. *Cell.* 74:1053–1064.

Matter, K., E.M. Yamamoto, and I. Mellman. 1994. Structural requirements and sequence motifs for polarized sorting and endocytosis of LDL and Fc receptors in MDCK cells. *J. Cell Biol.* 126:991–1004.

Mays, R.W., K.A. Siemers, B.A. Fritz, A.W. Lowe, G. van Meer, and W.J. Nelson. 1995. Hierarchy of mechanisms involved in generating Na/K-ATPase polarity in MDCK epithelial cells. *J. Cell Biol.* 130:1105–1115.

Meyer, C., D. Zizioli, S. Lausmann, E.L. Eskelinen, J. Hamann, P. Saftig, K. von Figura, and P. Schu. 2000. μ1A-adaptin-deficient mice: lethality, loss of AP-1 binding and rerouting of mannose 6-phosphate receptors. *EMBO (Eur. Mol. Biol. Organ.) J.* 19:2193–2203.

Molloy, S.S., E.D. Anderson, F. Jean, and G. Thomas. 1999. Bi-cycling the furin pathway: from TGN localization to pathogen activation and embryogenesis. *Trends Cell Biol.* 9:28–35.

Mostov, K., M.B. ter Beest, and S.J. Chapin. 1999. Catch the μ1B train to the basolateral surface. *Cell.* 99:121–122.

Nakamura, N., C. Rabouille, R. Watson, T. Nilsson, N. Hui, P. Slusarewicz, T.E. Kreis, and G. Warren. 1995. Characterization of a cis-Golgi matrix protein, GM130. *J. Cell Biol.* 131:1715–1726.

Nesterov, A., R.E. Carter, T. Sorkina, G.N. Gill, and A. Sorkin. 1999. Inhibition of the receptor-binding function of clathrin adaptor protein AP-2 by dominant-negative mutant μ2 subunit and its effects on endocytosis. *EMBO (Eur. Mol. Biol. Organ.) J.* 18:2489–2499.

Ohno, H., J. Stewart, M.C. Fournier, H. Bosshart, I. Rhee, S. Miyatake, T. Saito, A. Gallusser, T. Kirchhausen, and J.S. Bonifacino. 1995. Interaction of tyrosine-based sorting signals with clathrin-associated proteins. *Science.* 269:1872–1875.

Ohno, H., M.C. Fournier, G. Poy, and J.S. Bonifacino. 1996. Structural determinants of interaction of tyrosine-based sorting signals with the adaptor me-

dium chains. *J. Biol. Chem.* 271:29009–29015.

Ohno, H., T. Tomemori, F. Nakatsu, Y. Okazaki, R.C. Aguilar, H. Fölsch, I. Mellman, T. Saito, T. Shirasawa, and J.S. Bonifacino. 1999. Mu1B, a novel adaptor medium chain expressed in polarized epithelial cells. *FEBS Lett.* 449:215–220.

Orzech, E., K. Schlessinger, A. Weiss, C.T. Okamoto, and B. Aroeti. 1999. Interactions of the AP-1 Golgi adaptor with the polymeric immunoglobulin receptor and their possible role in mediating brefeldin A-sensitive basolateral targeting from the trans-Golgi network. *J. Biol. Chem.* 274:2201–2215.

Owen, D.J., and P.R. Evans. 1998. A structural explanation for the recognition of tyrosine-based endocytotic signals. *Science.* 282:1327–1332.

Rodriguez-Boulan, E., and S.K. Powell. 1992. Polarity of epithelial and neuronal cells. *Annu. Rev. Cell Biol.* 8:395–427.

Scheiffele, P., J. Peranen, and K. Simons. 1995. N-glycans as apical sorting signals in epithelial cells. *Nature.* 378:96–98.

Setou, M., T. Nakagawa, D.H. Seog, and N. Hirokawa. 2000. Kinesin superfamily motor protein KIF17 and mLin-10 in NMDA receptor-containing vesicle transport. *Science.* 288:1796–1802.

Sheff, D.R., E.A. Daro, M. Hull, and I. Mellman. 1999. The receptor recycling pathway contains two distinct populations of early endosomes with different sorting functions. *J. Cell Biol.* 145:123–139.

Simons, K., and E. Ikonen. 1997. Functional rafts in cell membranes. *Nature.* 387:569–572.

Simpson, F., N.A. Bright, M.A. West, L.S. Newman, R.B. Darnell, and M.S. Robinson. 1996. A novel adaptor-related protein complex. *J. Cell Biol.* 133: 749–760.

Sönnichsen, B., S. De Renzis, E. Nielsen, J. Rietdorf, and M. Zerial. 2000. Distinct membrane domains on endosomes in the recycling pathway visualized by multicolor imaging of Rab4, Rab5, and Rab11. *J. Cell Biol.* 149:901–914.

Stoorvogel, W., V. Oorschot, and H.J. Geuze. 1996. A novel class of clathrin-coated vesicles budding from endosomes. *J. Cell Biol.* 132:21–33.

Teuchert, M., W. Schafer, S. Berghofer, B. Hoflack, H.D. Klenk, and W. Garten. 1999. Sorting of furin at the trans-Golgi network. Interaction of the cytoplasmic tail sorting signals with AP-1 Golgi-specific assembly proteins. *J. Biol. Chem.* 274:8199–8207.

Wan, L., S.S. Molloy, L. Thomas, G. Liu, Y. Xiang, S.L. Rybak, and G. Thomas. 1998. PACS-1 defines a novel gene family of cytosolic sorting proteins required for trans-Golgi network localization. *Cell.* 94:205–216.

Yeaman, C., K.K. Grindstaff, and W.J. Nelson. 1999. New perspectives on mechanisms involved in generating epithelial cell polarity. *Physiol. Rev.* 79: 73–98.

Zhu, Y., L.M. Traub, and S. Kornfeld. 1999. High-affinity binding of the AP-1 adaptor complex to trans-golgi network membranes devoid of mannose 6-phosphate receptors. *Mol. Biol. Cell.* 10:537–549.

Zizioli, D., C. Meyer, G. Guhde, P. Saftig, K. von Figura, and P. Schu. 1999. Early embryonic death of mice deficient in γ-adaptin. *J. Biol. Chem.* 274: 5385–5390.